SUPPORTING INFORMATION

Chinese Journal of Structural Chemistry

Versatile Inorganic Oligomer-based Photochromic Spiropyrane Gels

Jiajia Song[1], Wei Duan[1], Yun Chen[1]* and Xiangyang Liu[2,3]*

[1]*State Key Laboratory of Chemo/Biosensing and Chemometrics, College of Chemistry and Chemical Engineering, Hunan University, Changsha 410082, China*

[2]*College of Ocean and Earth Sciences, College of Materials, College of Physical Science and Technology, State Key Laboratory of Marine Environmental Science (MEL), Research Institute for Biomimetics and Soft Matter, Xiamen University, Xiamen 361005, China*

[3]*Department of Physics, National University of Singapore, 2 Science Drive 3, Singapore 117542, Singapore*

Corresponding authors. Emails: ychen@hnu.edu.cn (Yun Chen) and liuxy@xmu.edu.cn (Xiangyang Liu)

SUPPORTING INFORMATION

Chinese Journal of Structural Chemistry

n TABLE OF CONTENTS

Section 1. Synthesis and Characterization of Spiropyran Calcium Ionic Oligomers

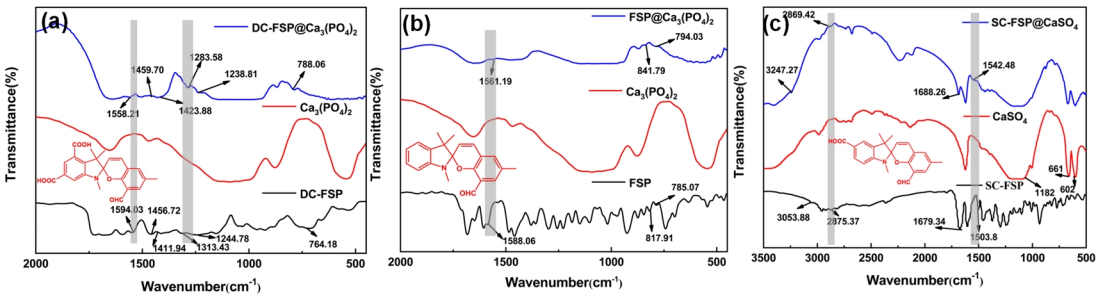

Figure S1. FTIR spectra of (a) DC-FSP@$Ca_3(PO_4)_2$, (b) FSP@$Ca_3(PO_4)_2$ and (c) SC-FSP@$CaSO_4$ oligomers.

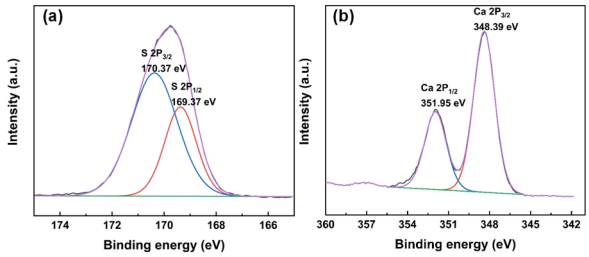

Figure S2. XPS spectra S2p (a) and Ca2p (b) of SC-FSP@$CaSO_4$ oligomers.

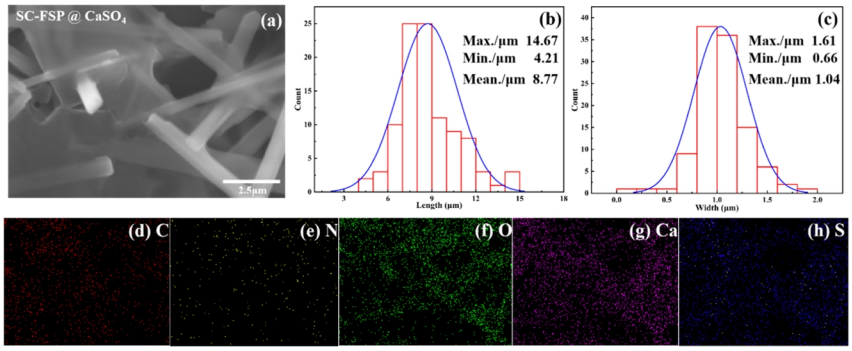

Figure S3. Scanning electron microscope image (a) and elemental mapping results of SC-FSP@$CaSO_4$ oligomers. (d) C, (e) N, (f) O, (g) Ca and (h) S. The length (b) and width (c) size distributions of SC-FSP@$CaSO_4$ were obtained by statistical analysis of more than 100 samples in the SEM image.

Section 2. Effect of Ca^{2+} on the Photochromic Behavior of Spiropyran Molecules

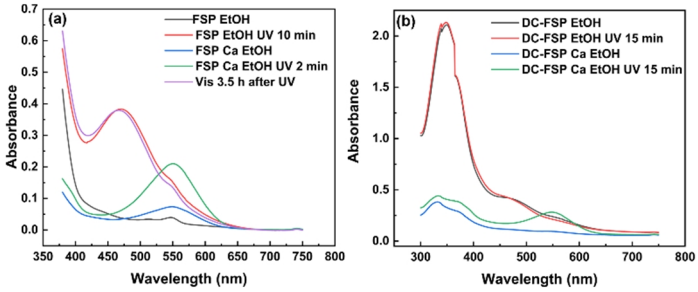

Figure S4. The effect of Ca^{2+} (30 mM) on the absorption spectra of (a) FSP (25.76 μM) and (b) DC-FSP (25.76 μM) in ethanol solution.

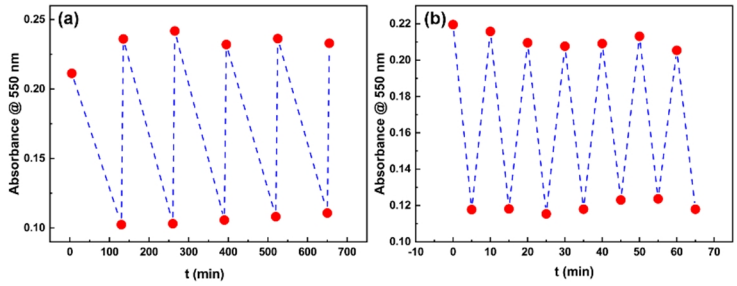

Figure S5. The fatigue resistance test in Ca^{2+} ethanol solution. (a) FSP irradiated alternately with UV for 5 min and Vis for 125 min. (b) DC-FSP irradiated alternately with UV for 5 min and Vis for 5 min.

Section 3. Study on the Photochromic Properties of Spiropyran Calcium Ionic Oligomers

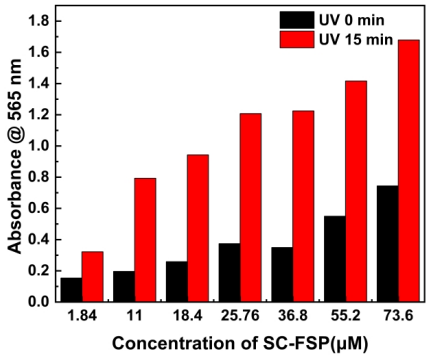

Figure S6. Optimization of SC-FSP concentration in order to prepare $(Ca_3(PO_4)_2)_n$ oligomers with optimum photochromic behavior.

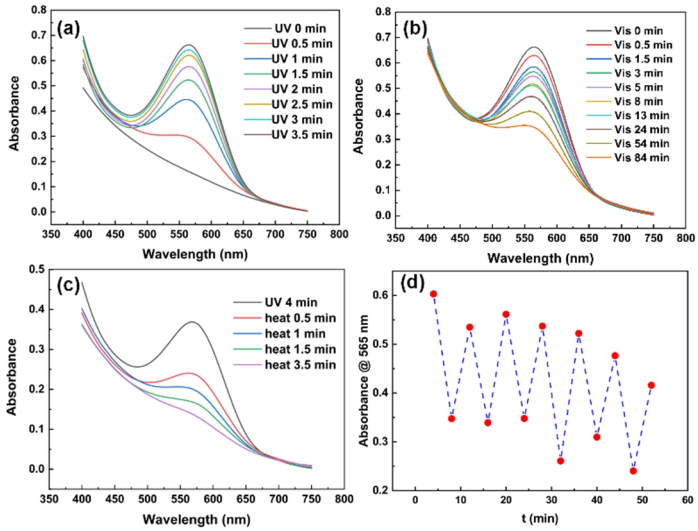

Figure S7. Photo-response behavior of SC-FSP@$Ca_3(PO_4)_2$ original oligomer solution. The time-dependent absorption spectra at 565 nm irradiated with ultraviolet light (a), visible light (b) and heated in a water bath at 50 °C (c). (d) Photodegradation-durability of the SC-FSP@$Ca_3(PO_4)_2$ original oligomer solution by alternately irradiating with UV for 4 min and heating in a 50 °C water bath for 4 min.

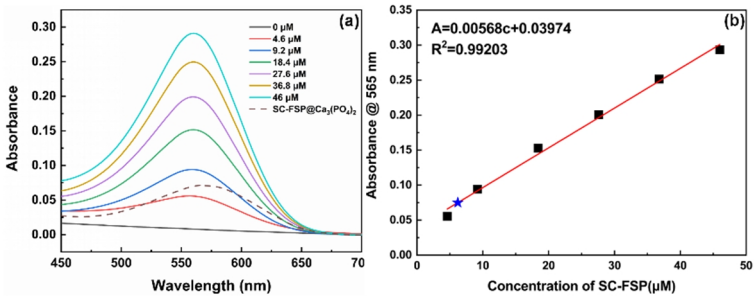

Figure S8. The embedding amount of SC-FSP in colloidal SC-FSP@$Ca_3(PO_4)_2$ oligomers calculated by UV-Vis absorption spectroscopy. (a) The absorption spectra of SC-FSP with the concentration range of 0-46 μM in ethanol solution containing 15 mM Ca^{2+}. The dotted line represents the absorption spectrum of residual SC-FSP in the supernatant of colloidal oligomers after centrifugation. The content of spiropyrans embedded in the colloidal oligomer is determined by subtracting the remaining content in the supernatant from the total spiropyrans content. (b) The standard curve is drawn by the function of the absorbance of SC-FSP at 565 nm and the concentration. The blue pentagram represents the residual SC-FSP content in the supernatant. Finally, the content of spiropyrans (SC-FSP) embedded in colloidal oligomers is determined to be 93.8% of the total content.

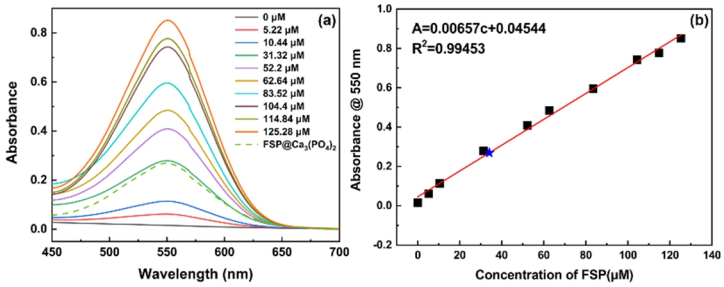

Figure S9. The embedding amount of FSP in colloidal FSP@$Ca_3(PO_4)_2$ oligomers calculated by UV-Vis absorption spectroscopy. (a) The absorption spectra of FSP with the concentrations range of 0-125 μM in ethanol solution containing 15 mM Ca^{2+}. The dotted line represents the absorption spectrum of residual FSP in the supernatant of colloidal oligomers after centrifugation. (b) The standard curve is drawn by the function of the absorbance of FSP at 550 nm and the concentration. The blue pentagram represents the residual FSP content in the supernatant. Finally, the content of spiropyrans (FSP) embedded in colloidal oligomers is determined to be 65.9% of the total content.

Table S1. Content Analysis of Spiropyrans Integrated into $Ca_3(PO_4)_2$ Oligomers by UV-Vis Spectroscopy

Spiropyran species	Calibration curve formulas	The absorbance at λ_{max} of residual spiropyrans in the supernatant	Concentration of residual spiropyrans in the super-natant (μM)	Percentage of spiropyrans embedded in oligomers in total content (%)
FSP	$A = 0.00657c + 0.04544$	0.2693	34.07	65.9
SC-FSP	$A = 0.00568c + 0.03974$	0.0750	6.21	93.8
DC-FSP		≈ 0	≈ 0	≈ 100

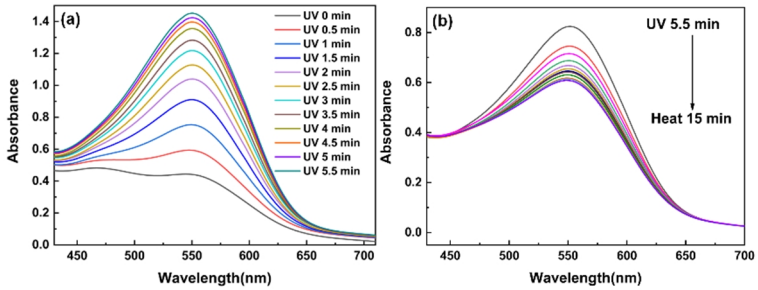

Figure S10. Photo-response behavior of colloidal DC-FSP@$Ca_3(PO_4)_2$ oligomers ($C_{DC\text{-}FSP}$ = 49.2 μM). The time-dependent absorption spectra at 550 nm irradiated with ultraviolet light (a) and heated in a water bath at 50 °C (b)

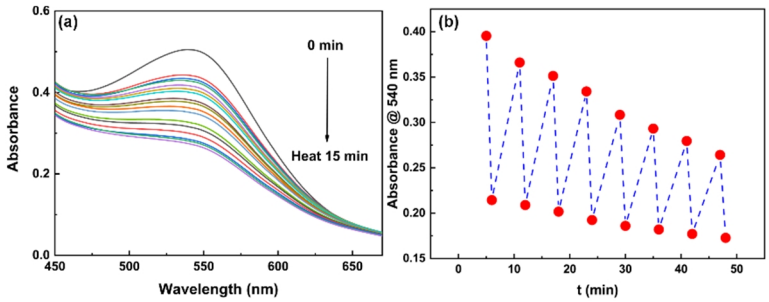

Figure S11. Photo-response behavior of colloidal FSP@$Ca_3(PO_4)_2$ oligomers (C_{FSP} = 125.28 μM). (a) The time-dependent absorption spectra at 540 nm heated in a water bath at 50 °C. (b) Photodegradation-durability by alternately irradiating with UV for 5 min and heating in a 50 °C water bath for 15 min.

Table S2. The Coloration and Discoloration Rate Equations and Kinetic Parameters of Spiropyran SC-FSP under UV and Vis Radiation or Heating in Different Matrix Environments (Original $Ca_3(PO_4)_2$ Oligomer Solution, Colloidal $Ca_3(PO_4)_2$ Oligomers and Ethanol Solution with 30 mM Ca^{2+}).

Condition		Equation	R^2	K_C (S^{-1})	$T_{1/2}$ (S)
original oligomer solution	SP→MC UV	$\ln\frac{A_t - A_e}{A_0 - A_e} = -0.01632t + 0.11394$	0.98482	1.63×10^{-2}	43
	MC→SP heated at 50 °C	$\ln\frac{A_t - A_e}{A_0 - A_e} = -0.02264t - 0.04201$	0.98486	2.26×10^{-2}	31
colloidal oligomers with $n(Ca^{2+}):n(TEA)$ = 1:20	SP→MC UV	$\ln\frac{A_t - A_e}{A_0 - A_e} = -0.01472t + 0.37819$	0.98386	1.47×10^{-2}	47
	MC→SP heated at 50 °C	$\ln\frac{A_t - A_e}{A_0 - A_e} = -0.00411t - 0.12125$	0.97787	4.11×10^{-3}	169
colloidal oligomers with $n(Ca^{2+}):n(TEA)$ = 1:5	SP→MC UV	$\ln\frac{A_t - A_e}{A_0 - A_e} = -0.01645t + 0.48585$	0.98124	1.65×10^{-2}	42
	MC→SP heated at 50 °C	$\ln\frac{A_t - A_e}{A_0 - A_e} = -0.01272t - 0.35116$	0.98512	1.27×10^{-2}	55
ethanol solution with 30 mM Ca^{2+}	SP→MC UV	$\ln\frac{A_t - A_e}{A_0 - A_e} = -0.0279t + 0.03722$	0.99699	2.79×10^{-2}	25
	MC→SP Vis	$\ln\frac{A_t - A_e}{A_0 - A_e} = -0.09576t + 0.05041$	0.99744	9.58×10^{-2}	7

Section 4. Naked Eye Detection and Mechanism Study of Liquid and Gaseous Hydrazine on the Paper and Soft Substrates.

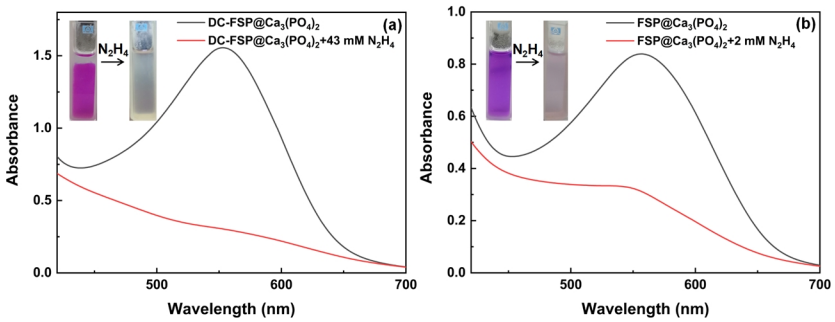

Figure S12. UV-Vis absorption spectra of (a) DC-FSP and (b) FSP (*C* = 100 μM) with or without hydrazine in original $Ca_3(PO_4)_2$ oligomers solution. The illustrations show the photos of spiropyrans@$Ca_3(PO_4)_2$ oligomers solution with or without hydrazine under natural light.

Paper Substrate Sensor: Naked Eye Detection of Hydrazine in Solution. The filter paper was used as the substrate for the construction of liquid hydrazine sensor. Spiropyrans were coated on the filter paper by soaking the filter paper strips in ethanol solutions of SC-FSP, DC-FSP and FSP (9.2 mM) with or without Ca^{2+} for 2 min and drying, respectively. Then, hydrazine ethanol solutions with different concentrations were dropped onto the filter paper and dried naturally. The identification of hydrazine concentrations in ethanol solution was simply realized by the color changes of filter paper under visible light and UV light.

Colloidal Flexible Substrate Sensor: Naked Eye Detection of Hydrazine Vapor. The SC-FSP@$Ca_3(PO_4)_2$ oligomer colloid ($C_{SC\text{-}FSP}$ = 25.76 μM) was obtained by centrifugation. Under UV light stimulation, the spiropyrans loaded in the colloid were photoisomerized to ring-opened MC form and the colloid was induced to turn purple. Then the purple colloid was smeared on the foam and placed on the top of the bottles containing different concentrations of aqueous solution of hydrazine (3 mL, concentrations: blank, 0.1%, 1%, 5%, 10%, 15%, 20%, 30%, 40%, 70% and 100%) and other analyte aqueous solutions for one hour at room temperature. The color changes of colloid observed under visible and UV light were used for the detection of gaseous hydrazine.

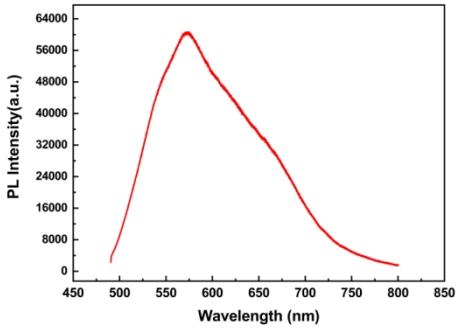

Figure S13. Solid state fluorescence spectra of SC-FSP@$Ca_3(PO_4)_2$ oligomer colloid (excitation wavelength: 488 nm).

Mechanism Study

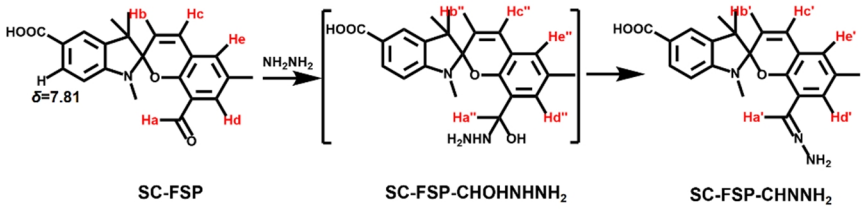

SC-FSP SC-FSP-CHOHNHNH$_2$ SC-FSP-CHNNH$_2$

Table S3. In the ^{1}H NMR Titration Spectra of SC-FSP and Different Equivalent N_2H_4, the Integral Area of the Proton at δ = 7.81 Is Taken as the Standard "1", and the Content Changes of Reactant [SC-FSP], Hemiaminal Intermediate and Final Product Hydrazone [SC-FSP-CHNNH$_2$] Are Tracked through the Integral Areas of Protons on the Double Bond of Pyran Ring and Formyl Group. The Relevant Integral Areas Are Shown in Table S3.

n(N_2H_4) /*n*(SC-FSP)	0	0.1	0.3	0.5	0.7	0.9
formyl proton (-chao) at δ = 9.94	0.88	0.72	0.46	0.18	0	0
hydrazone ha' at δ = 7.54	0	0	0.26	0.39	0.55	0.98
hc at δ = 7.10	0.98	0.79	0.57	0.22	0	0
hemiaminal hc" at δ = 7.025	0	0.18	0.23	0.42	0.42	0
hydrazone hc' at δ = 6.965	0	0	0.27	0.39	0.55	0.98
hb at δ = 5.925	0.97	0.78	0.51	0.21	0	0
hemiaminal hb" at δ = 5.84	0	0.17	0.27	0.40	0.43	0
hydrazone hb' at δ = 5.76	0	0	0.25	0.38	0.52	0.94

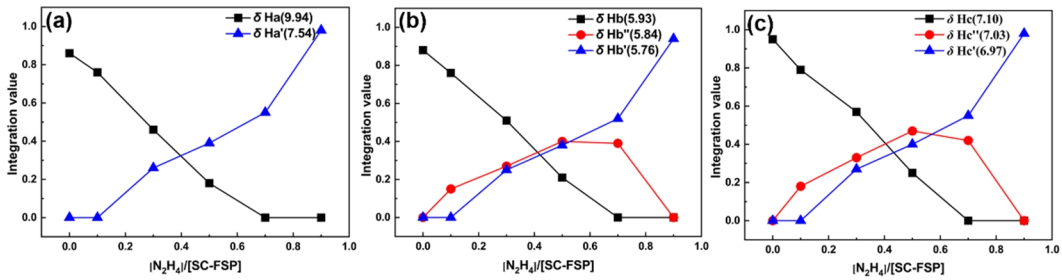

Figure S14. The content changes of protons on the double bond of pyran ring and formyl group in the reactant [SC-FSP], hemiaminal intermediate and final product hydrazone [SC-FSP-CHNNH$_2$] during the titration experiments of SC-FSP and different equivalent N_2H_4.

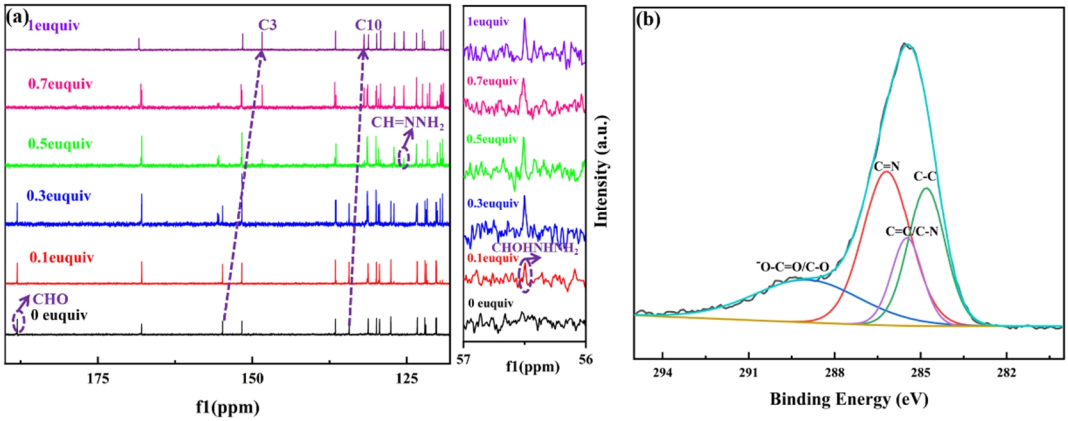

Figure S15. (a) Partial ^{13}C NMR spectra of SC-FSP (lowest) and the product of SC-FSP reacting with different equivalent N_2H_4 (solvent: DMSO-d_6). (b) XPS decomposition peak of C1s obtained by high-resolution scanning.

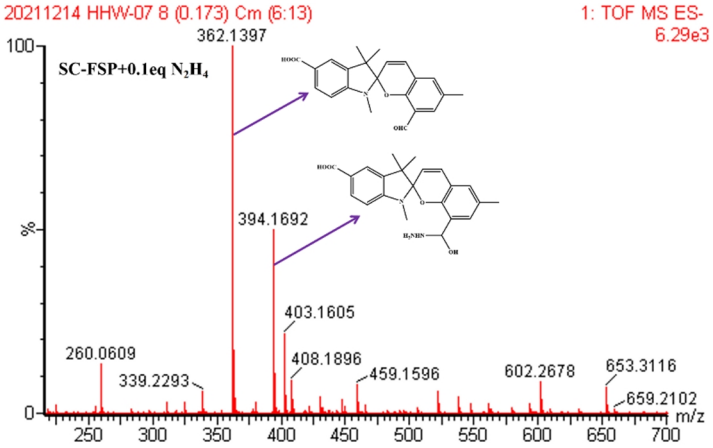

Figure S16. HRMS spectrum of the product of SC-FSP with 0.1 equiv. N_2H_4. Remaining reactant *m/z* $[M-H]^-$ calcd. for $C_{22}H_{20}NO_4$: 362.1471; found: 362.1397. Hemiaminal intermediate *m/z* $[M-H]^-$ calcd. for $C_{22}H_{24}N_3O_4$: 394.1845; found: 394.1692.

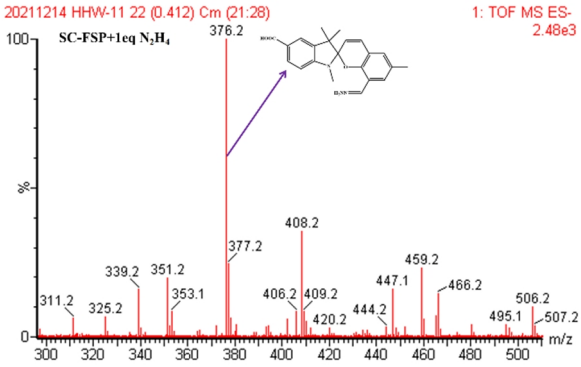

Figure S17. Mass spectrum of the product of SC-FSP with 1 equiv. N_2H_4. Final product hydrazone *m/z* $[M-H]^-$ calcd. for $C_{22}H_{22}N_3O_3$: 376.2; found: 376.2.

Section 5. Computational Study

Computational Method. The theoretical calculations of SC-FSP, hemiaminal intermediate [SC-FSP-CHOHNHNH$_2$] and the final product hydrazone [SC-FSP-CHNNH$_2$] were carried out by using Gaussian 09 software package. The geometric structure optimizations were performed at the DFT level with the B3LYP functional and 6-31+G (d, p) basis set. Considering the accuracy of geometric optimization and ensuring its minimum energy, the vibrational frequencies were calculated at the same theoretical level. The mPW1PW91/6-311+G (2d, p) method was used to compute the magnetic shielding tensor based on the optimized geometric structure. The chemical shifts of each hydrogen atom and carbon atom were calculated according to the formulas δ = (31.7217 - σ_{iso})/1.0580 and δ = (186.2534 - σ_{iso})/1.0496, respectively.

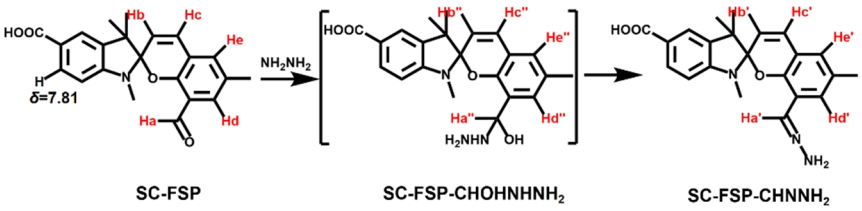

SC-FSP SC-FSP-CHOHNHNH$_2$ SC-FSP-CHNNH$_2$

Table S4. The Chemical Shifts of Hydrogen Atoms of SC-FSP, SC-FSP-CHOHNHNH$_2$ and SC-FSP-CHNNH$_2$ Calculated by mPW1PW91/6-311+G (2d, p) Method Are Compared with the Experimental Values in ^{1}H Spectra.

	SC-FSP					SC-FSP-CHOHNHNH$_2$			SC-FSP-CHNNH$_2$				
	Ha	Hb	Hc	Hd	He	Ha''	Hb''	Hc''	Ha'	Hb'	Hc'	Hd'	He'
calculated value	10.00	5.96	7.24	7.62	7.49	5.13	5.77	7.10	7.77	5.80	7.06	7.63	7.00
experimental value	9.94	5.925	7.10	7.32	7.36	Not find	5.84	7.025	7.54	5.76	6.965	7.33	6.88

Table S5. The Chemical Shifts of Carbon Atoms of SC-FSP and SC-FSP-$CHNNH_2$ Calculated by mPW1PW91/6-311+G (2d, p) Method Are Compared with the Experimental Values in ^{13}C Spectra.

Number	SC-FSP-CHO		SC-FSP-$CHNNH_2$	
	calculated value	experimental value	calculated value	experimental value
35	164.91	167.92	165.06	168.34
15	135.80	136.54	135.61	136.52
16	151.46	151.68	152.85	151.56
17	105.60	106.61	105.39	106.16
19	132.28	131.23	132.05	131.19
20	116.99	120.20	116.40	119.08
21	123.34	123.29	123.34	123.40
1	130.60	129.91	130.80	129.86
2	118.77	121.91	119.63	122.13
3	154.40	154.81	147.52	148.42
4	118.56	120.27	117.75	119.46
9	129.35	129.40	129.29	129.22
10	134.48	134.32	126.22	131.92
12	126.40	127.57	123.02	126.97
14	120.30	122.07	120.04	122.45
42	187.22	188.05	133.32	125.45
23	26.22	28.90	27.17	28.74
41	104.91	105.31	106.49	104.07
7	54.89	51.73	56.29	51.39
27	24.87	25.93	23.34	26.24
31	17.97	20.26	17.58	20.64
44	18.91	20.51	18.99	20.73

Section 6. Synthesis and Characterization of Spiropyrans

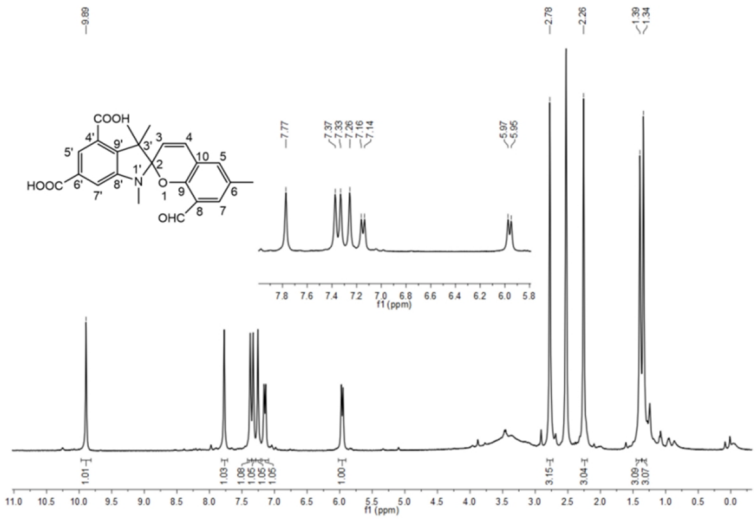

Figure S18. ^{1}H NMR spectrum of DC-FSP.

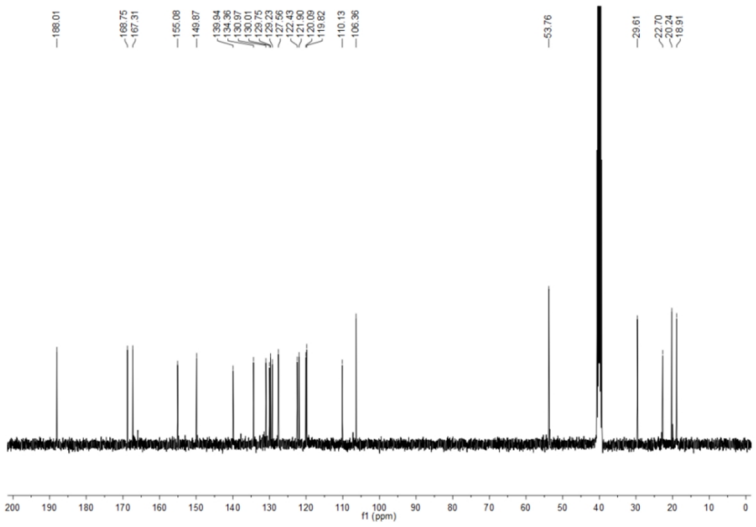

Figure S19. ^{13}C NMR spectrum of DC-FSP.

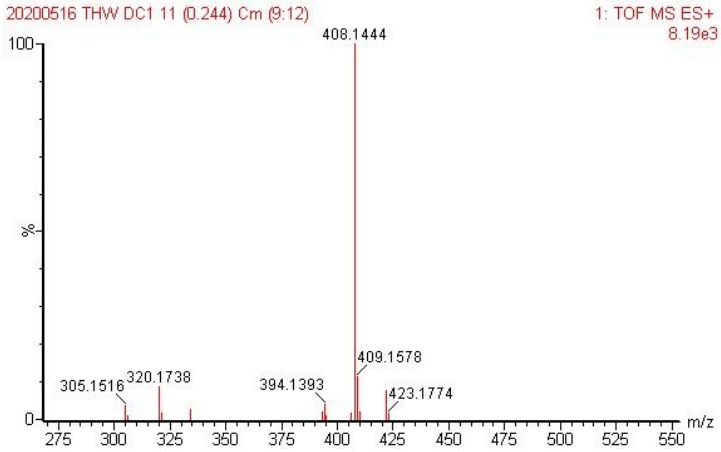

Figure S20. Mass spectra of DC-FSP.

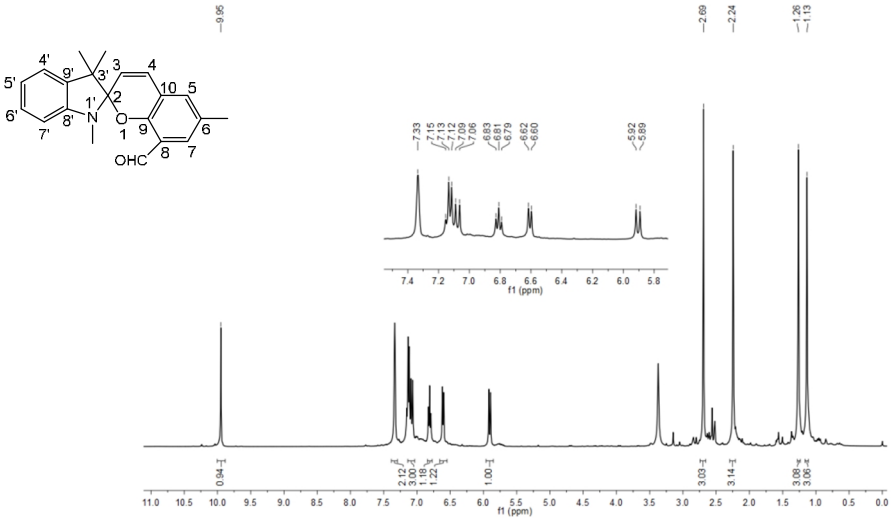

Figure S21. ^{1}H NMR spectrum of FSP.

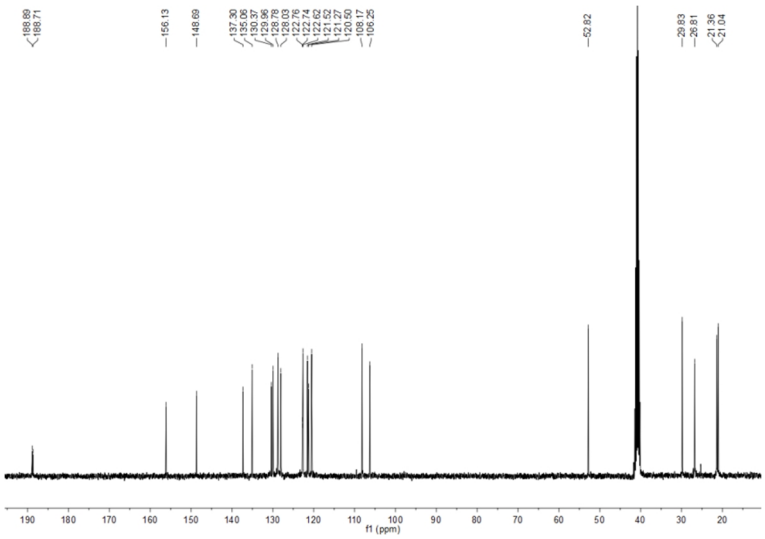

Figure S22. ^{13}C NMR spectrum of FSP.

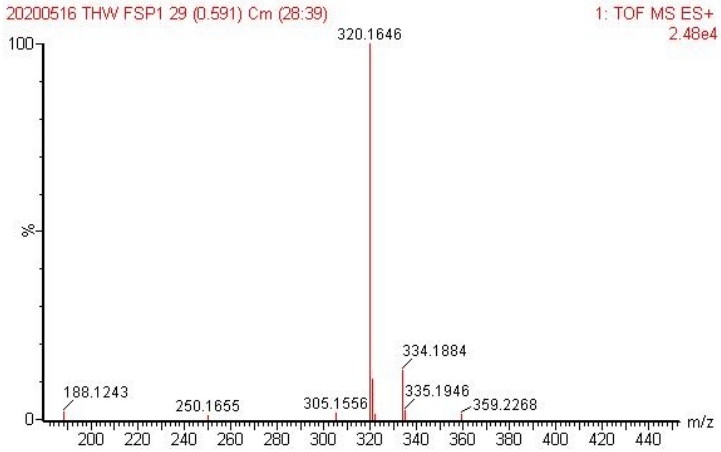

Figure S23. Mass spectra of FSP.

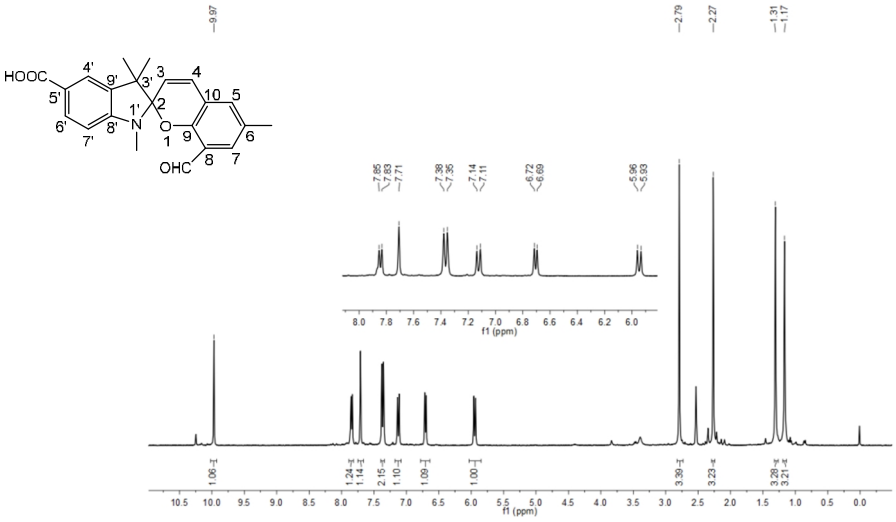

Figure S24. ^{1}H NMR spectrum of SC-FSP.

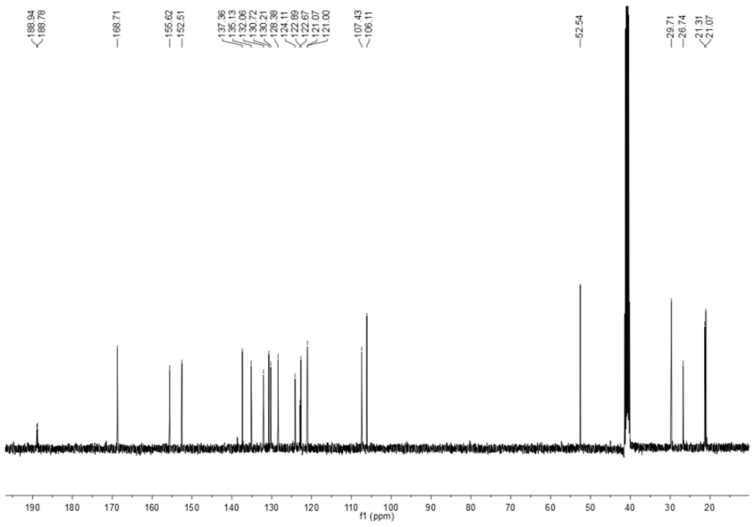

Figure S25. ^{13}C NMR spectrum of SC-FSP.

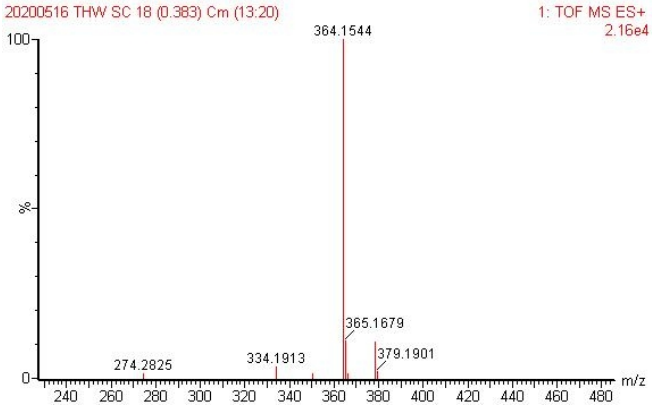

Figure S26. Mass spectra of SC-FSP.